Lowland Technology International date; Volume 22 (2): 200-2011
International Association of Lowland Technology (IALT): ISSN 1344-9656

Research Paper

Determination of shear wave velocity by using multichannel analysis of surface wave and borehole measurements: A case study in Ho Chi Minh City

N.N.K. Ngan [1], D.V. Luu [2] , N.T. Van [3] and T.D. Tap[4]

ARTICLE INFORMATION

Article history:

Received: 04 October, 2019
Received in revised form: 20 November, 2019
Accepted: 25 November, 2019
Publish on: 06 September, 2020

Keywords:

Stiffness of soil
MASW
V_S
V_{S30}
downhole

ABSTRACT

The soil characterization of the residential development project located in Ho Chi Minh City (HCMC) was conducted by using multichannel analysis of surface wave (MASW) and downhole measurements. The obtained results of both methods indicate that the soils within the depth range of 0–30 m were divided into three layers including (i) the filled soil with shear wave velocity (V_S) values of 75–93 m/s, (ii) the silty clay with V_S of 61–200 m/s, and (iii) the firm layer soil with V_S of 250–415 m/s. The V_{S30} values estimated by using the MASW, downhole, and empirical correlation methods are in the range of 150–152, 137–161, 126–171 m/s, respectively. Accordingly, the study area is well classified as class E according to National Earthquake Hazards Reduction Program guidelines (NEHRP). The MASW results are in good agreement with those obtained by using the downhole measurements with the average relative difference of 3–4%. This study represents a first attempt of using the MASW method to evaluate the stiffness of soil around HCMC areas and the results obtained from this method and correlation between standard penetration test (SPT)-N and V_S can contribute a further detailed understanding of geophysical features in the HCMC area.

1. Introduction

Ho Chi Minh City (HCMC), the most active city and economic center of Viet Nam, covers an area of 2,095 km^2 with the highest population density (around 8 million people). District 2 locating at the gateway in the northeast HCMC is being the large building construction projects at the new planned city of Thu Thiem to be a center of urban, economy, and finance in the near future (Nguyen and Phienwej, 2016; Nguyen et al., 2016). It is planned to construct for hundreds of high-rise buildings, a residential accommodation for 130,000 residents, and a leisure center for one million visitors. Currently, many large construction projects have been constructing or will be constructed, and thus numerous geological and geophysical surveys have been conducted here.

For the geophysical surveys, the shear wave velocity (V_S) is one of the key parameters to examine the stiffness of soil. The borehole measurements (downhole and crosshole methods) have been performed intensively to estimate V_S (Xia et al., 2002; Park et al., 2007; Rahman et al., 2017). In Viet Nam, those methods have been utilized

[1] Corresponding author, PhD student, Geophysics Department, Faculty of Physics and Engineering Physics, University of Science, Viet Nam National University Ho Chi Minh City, 227 Nguyen Van Cu, District 5, Ho Chi Minh, Viet Nam, nnkngan@hcmus.edu.vn
[2] Lecturer, Geophysics Department, Faculty of Physics and Engineering Physics, University of Science, Viet Nam National University Ho Chi Minh City, 227 Nguyen Van Cu, District 5, Ho Chi Minh, luudv44@gmail.com
[3] Associate Professor, Geophysics Department, Faculty of Physics and Engineering Physics, University of Science, Viet Nam National University Ho Chi Minh City, 227 Nguyen Van Cu, District 5, Ho Chi Minh, ntvan@hcmus.edu.vn
[4] Corresponding author, Lecturer, Faculty of Materials Science and Technology, University of Science, Viet Nam National University Ho Chi Minh City, 227 Nguyen Van Cu, District 5, Ho Chi Minh, Viet Nam, tdtap@hcmus.edu.vn
Note: Discussion on this paper is open until March 2021

at many areas to measure the seismic velocities and elastic parameters of soil in the construction projects such as the German House (District 1, HCMC) (Nguyen et al., 2014), the Samsung Electronics CE Complex at Saigon High Tech Park (District 9, HCMC) (Nguyen and Vo, 2015), the thermal power plant (Soc Trang province) (Nguyen et al., 2016), the residential development at Thu Thiem area (District 2, HCMC) (Do and Vo, 2017), and the solar power plant at My Son (Ninh Thuan province) (Do et al., 2018). The invasive techniques cited above, however, are costly and time consuming and require the boreholes at the survey areas (Xia et al., 2000, 2002).

Recently, multichannel analysis of surface wave (MASW) has been exhibited as a potential method to investigate the stiffness of soils. This method, developed by Park et al., has an extensive history at Kansas geological survey belong to University of Kansas dating from the 1990s (Park et al., 1999). The MASW method is based on the fact that the surface waves are dispersive in the inhomogeneous medium, whereas the phase velocities depend on the frequency. Consequently, the dispersion curve of the surface wave could be easily identified on the dispersion image. Besides that, noise and body waves could be identified, isolated, and rejected in data analysis (Madun et al., 2016). Other advantages of the MASW method include both speed of data acquisition and cost-effectiveness (Xia et al., 2000, 2002). Although the MASW method possesses several advantages as presented above, there are no reports using this method in the HCMC area and even in Viet Nam. Accordingly, using the MASW survey as an alternative method to provide the advance information about the stiffness of the soil over the whole country is necessary. As a starting point to conduct above purposes, in the present study, we have utilized the MASW method to investigate the stiffness of the soil at the residential development project located at District 2 in HCMC. The results of the shear wave velocity profiles by using the MASW method could be compared to those obtained by the downhole measurements and empirical correlation between V_S and standard penetration test (SPT)-N values. On the basic of the results of shear wave velocity profiles, the stiffness of the soil is classified and evaluated. Note that the results of this study can contribute a further detailed understanding of geophysical features in the HCMC area.

2. Experimental

2.1 Geology of the study area

The subsurface geological materials of HCMC are divided into two main lithological units including (i) Pre-Cenozoic vertical sediment basement formed by Jura sedimentary rock and Lave Mesozoic pluton-volcanic complex within a depth of 330 m and (ii) Late Miocene-Quaternary sediment overlay structure having a thickness of 300 m. Moreover, this area consists of Holocene and Pleistocene sediment structural sub-units with thickness ranging from several and ten to forty and several hundred meters, respectively (Nguyen, 2004; Do et al., 2018; Vu and Do, 2018). The geology features at District 2 exhibit as the class of Holocene salt marsh and river marsh deposits. This region is quite sunken with the average elevation of 1 m above mean sea level (Nguyen, 2004; Do et al., 2018; Vu and Do, 2018). In areas along the rivers, the soft dark silty clay layers are located under the surface soil, causing many landslides. Below that, the gravel clay and sandy layers are formed alternately (Nguyen, 2004; Do et al., 2018; Vu and Do, 2018).

2.2 The MASW survey

Fig. 1 presents a map of study area (about 16,000 m^2) with positions of fourteen boreholes (bold numbered dots) locating at latitude 10º46’N and longitude 106º45’E. The MASW survey was performed at boreholes of BH7 and PBH2. In this work, the active MASW mode was utilized by placing the multiple receivers (geophones) along a survey line with single shots (Eker et al., 2012). The distance between BH7 and PBH2 is 25.3 m and the diameter of each borehole is around 110 mm.

Fig. 2 shows the schematic diagram of the MASW survey. Twenty-four vertical geophones (G1-G24) with frequency of 4.5 Hz connected to a Seistronix RAS-24 seismograph were used to record the wave signals. Geophone spacing, sampling rate, and record length were respectively set at 2 m, 125 ms, and 2 s (Trupti et al., 2012). The borehole locates between the 12^{th} and 13^{th} geophones. The source offsets were sequentially set at 6 and 16 m to the left and right of the receiver system. In this study, a 9-kg sledgehammer was employed to knock on the metal plate to generate the seismic waves. The detailed analysis of the MASW-method data is conducted as the followings (Abreu et al., 2016). (i) The seismic records were loaded into the copyright PS software (Park Seismic LLC) to display and transform the raw data to phase velocity-frequency spectrum to get the dispersion images. For two boreholes of BH7 and PBH2, the frequency and phase velocity were set in the range of 1−30 Hz and 1−500 m/s, respectively. (ii) Four dispersion images from four records for each borehole were combined to obtain each stacked dispersion image. This process could maximize the robustness of data, and thus minimize the adverse influence of the near-field effects and average the lateral variation of the subsurface velocity model (Park et al., 1999; Hartantyo et al., 2014). (iii) The peak values were selected from the dispersion image to generate the dispersion curve, which is then presented as a plot of phase velocity versus frequency. The shear wave velocity profile was calculated using an iterative inversion process with data of the dispersion curve as input. A nonlinear least square technique provides an automation in the inversion process to generate the 1D V_S profile, which shows the distribution of shear wave velocity of the near-surface soils (Nguyen et al., 2015).

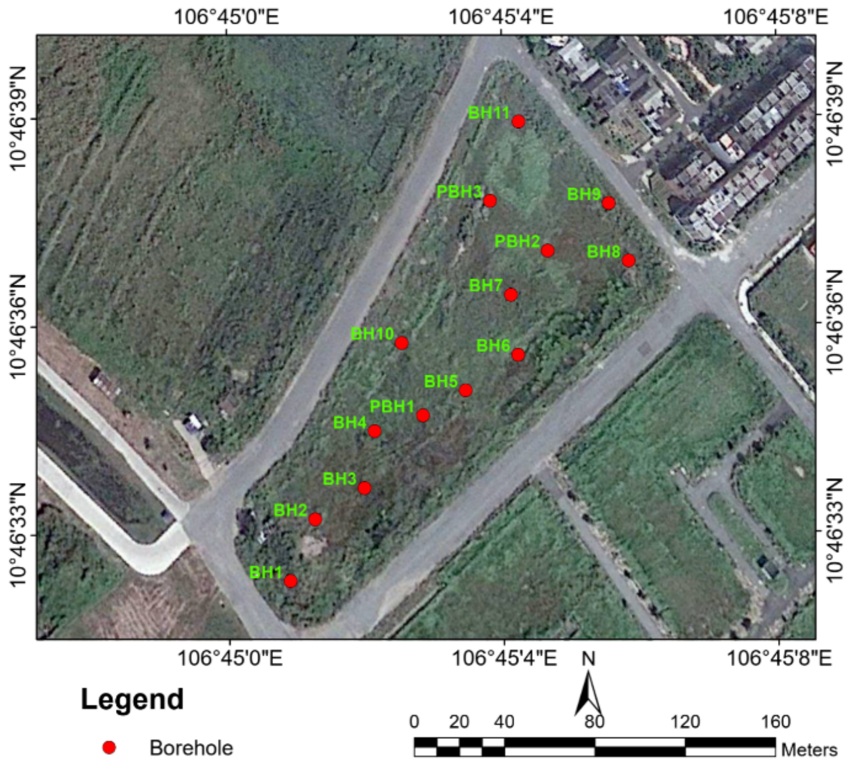

Fig. 1. A map of study area with positions of fourteen boreholes (numbered dots). The MASW measurements were conducted at two sites of BH7 and PBH2.

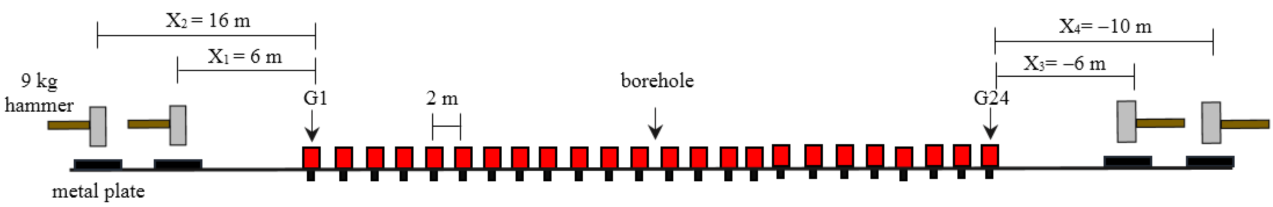

Fig. 2. The schematic diagram of the MASW survey. The length of the MASW array is 46 m and X_i is source offsets.

2.3 The downhole survey

The downhole survey was carried out at all fourteen boreholes having N values from SPT. The detailed procedures are carried out as follows (Do and Vo, 2017). (i) A hammer and a metal plate are set closely to the mouth of borehole (2–5 m), whereas the three-component geophone is lowered into the borehole to detect the seismic waves at different depths. (ii) A hammer is used to strike on the metal plate to generate the seismic waves and the received signal of the secondary wave was checked on the wave diagram. (iii) The sensor is moved down to another 3-m depth interval and repeat steps (i) and (ii). The first arrival time of P wave can be identified as the first departure of the static horizontal receiver trace after T = 0 s. The shear wave is identified on the seismic signature as a sudden increase in amplitude, which is several times higher than that of the P-wave. The shear wave velocity is determined at each depth interval using the arrival time of the shear wave and the corresponding depth (Nguyen et al., 2014; Do and Vo, 2017).

2.4 The average shear wave velocity

V_{S30}, which is defined as an average shear wave velocity of soils within the depth range of 0–30 m (advised by the National Earthquake Hazards Reduction Program (NEHRP)), is used as an index for characterization of seismic site. The V_{S30} can be determined by the following equation (Haque et al., 2013; Araffa et al., 2014; Raef et al., 2015; Rehman et al., 2016):

$$V_S = \frac{\sum_{i=1}^{n} d_i}{\sum_{i=1}^{n} V_{S_i}} \quad [1]$$

where d_i and V_{Si} are thickness and shear wave velocity of the i^{th} layer, respectively.

3. Results and discussion

Fig. 3 shows the MASW-method data, which was acquired by using 24-traces with different source offsets and orientations at BH7 (3a-3d) and PBH2 (3e-3h) sites. Rayleigh wave phase velocity is extracted from the field data for the inversion process, in which multichannel records in time-space (t-x) domain were transformed into frequency-wave number (f-k) domain or frequency-phase velocity (f-C) domain (Banab and Motazedian, 2010; Thitimakorn, 2010; Pamuk et al., 2017).

Fig. 4 depicts the results of dispersion images at sites of BH7 (4a) and PBH2 (4b) stacked from four single dispersion images. The stacking process was conducted

3.1 Dispersion images

by combining the dispersion images with different shot gathers in order to suppress ambient noise and increase the resolution, which leads to increase the depth of investigation (Banab and Motazedian, 2010). The two dispersion images exhibit more distinctive dispersion curves with very strong accumulated energy (Pamuk et al., 2017). The dispersion curves of the two boreholes show relatively similar; namely, with high frequency of 15–30 Hz, the phase velocities are approximately 100 m/s. The phase velocities decrease and increase in the frequency range of 5–15 Hz and with lower frequency than 5 Hz, respectively.

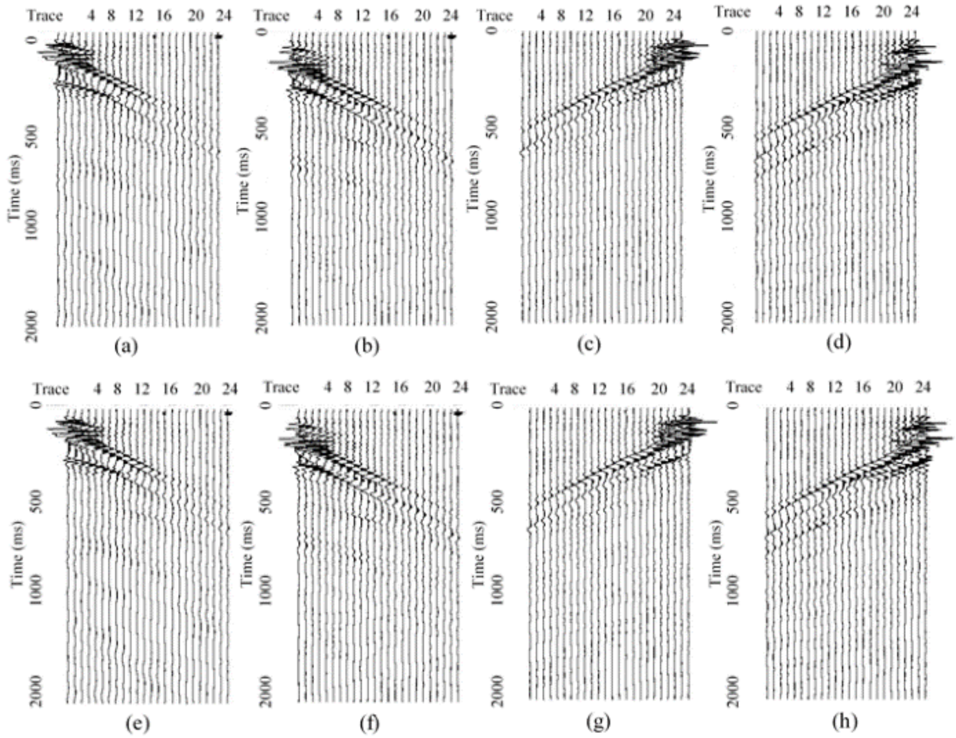

Fig. 3. Seismic records with different source offsets and orientations at two borehole sites of BH7 ((a) X_1 = 10 m, (b) X_2 = 16 m, (c) X_3 = -10 m, (d) X_4 = -16 m) and PBH2 ((e) X_1 = 10 m, (f) X_2 = 16 m, (g) X_3 = -10 m, (h) X_4 = -16 m).

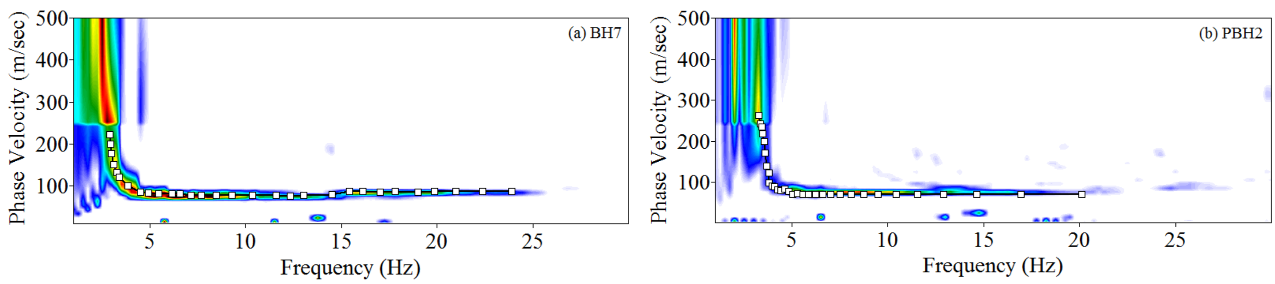

Fig. 4. The dispersion images stacking from different source orientations and source offset records for two sites of BH7 and PBH2.

3.2 The 1D V_S profiles

Fig. 5 represents the 1D V_S profiles as a function of depth for two boreholes of BH7 and PBH2 obtained by using the MASW method. The soils for two boreholes are divided into twelve layers within a depth of 30 m. At borehole of BH7 (Fig. 5a), the value of V_S at the first layer (1.5 m in thickness) is approximately 93 m/s. In the depth range of 1.5–9 m (the second to fifth layers), the V_S decreases slightly from 84 to 68 m/s. The V_S increases approximately from 157 to 400 m/s with higher depth range than 9 m (the sixth to half space (H/S) layers). At borehole of PBH2 (Fig. 5b), the value of V_S of the first layer (1.5 m in thickness) is around 75 m/s. The V_S values increase from 71 and 200 to 80 and 415 m/s in the second-fifth and sixth-H/S layers, respectively. Although the V_S values measured at two sites (BH7 and PBH2) are slightly different, the changes of V_S values are similar. This similar behavior can be explained from the fact that the two boreholes are relative close to each other (Fig. 1), leading to the similar environmental geology.

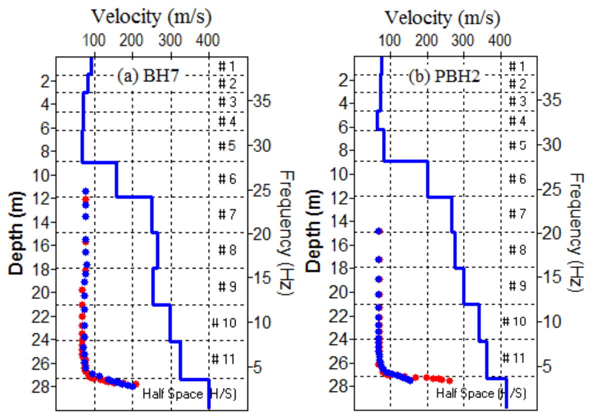

Fig. 5. The 1D V_S profiles as a function of depth at two sites of BH7 and PBH2 obtained by using the MASW method.

3.3 Empirical correlation between V_S and SPT-N

As presented in Section 3.2, the MASW method provides the shear wave velocity with depth, but borehole characterization does not fully understand without knowledge of subsurface stratum and soil type. Accordingly, SPT is intensively used to evaluate the strength of soil. The correlation between V_S and SPT-N is determined by using the following equation (Kirar et al., 2016; Madun et al., 2016; Rahman et al., 2016):

$$V_S = aN^b \quad [2]$$

where N being SPT-N values and a and b being regression coefficients, which are inversely proportional to each other. Empirical functions for this correlation have been proposed previously in many works as presented in Table 1. To date, limited reports have been made to develop such a relation for soil sites in the HCMC area. Consequently, in this study, we have employed respectively 137 and 113 data pairs of V_S measured by the downhole method and SPT-N values estimated from fourteen boreholes to derive empirical correlations for all soils and all clayey soils (Fig. 6). The measured SPT-N values varied from 1 and 5 to 40 for all soils and all clayey soils, respectively, which were directly used here for correlation. The proposed correlations between V_S and SPT-N are estimated by the following equations:

$$V_S = 76.45N^{0.468} \ (R^2 = 0.935) \text{ for all soils} \quad [3]$$
$$V_S = 108.31N^{0.355} \ (R^2 = 0.634) \text{ for all clayey soils} \quad [4]$$

Due to the limited available spatial data for SPT-N, the empirical correlations for the sand and silt soils have not been developed. As the results showed in Table 1, for all soils, the values of a and b are in the range of 22–137.15 and 0.24–0.85, respectively. For all clayey soils, the values of a and b are respectively in the range of 27–184.2 and 0.17–0.73. Thus, the V_S in this study exhibits the intermediate value in comparison with those in Table 1. The values of a and b for all soils and all clayey soils showed in Table 1 vary in the wide range, leading to the assumption that the specific geological features of other previous study areas were much different. Moreover, the quantity of analyzed data, the SPT procedures, and the different methods for shear wave velocity measurements could be other reasons causing the variations of a and b values showed in Table 1. Based on the results in this study, it is observed that the empirical equations for all soils and all clayey soils differ considerably; namely, the values of R^2 and a and b for all clayey soils (0.634; 108.31; 0.355) are respectively lower and higher than those (0.935; 76.45; 0.468) for all soils (equations (3) and (4)). Thus, the soil type at the study area has a significant effect on the empirical correlations. The similar results were also observed in some previous works (Yokota et al., 1991; Anthanasopoulos, 1995; Raptakis et al., 1995; Pitilakis et al., 1999; Anbazhagan et al., 2013; Sun et al., 2013; Rahman et al., 2018).

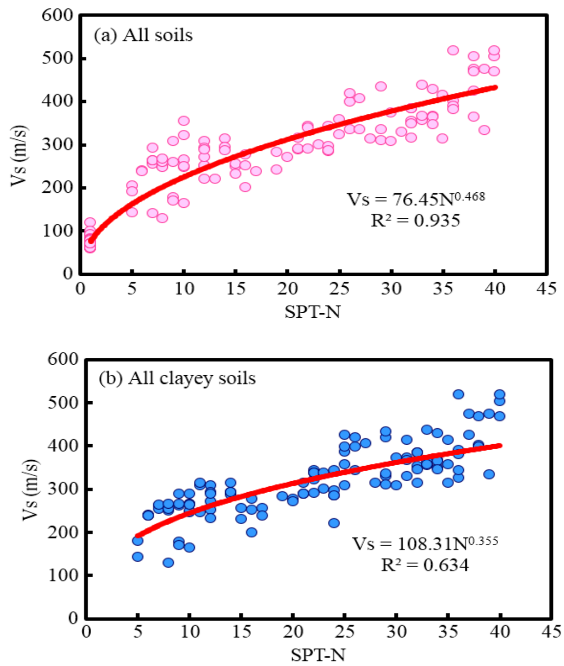

Fig. 6. Empirical correlation between V_S and SPT-N in the study area for (a) all soils and (b) all clayey soils.

Table 1. Empirical correlation between V_S and SPT-N of this study and some previous works.

Anthor(s)	Vs (m/s)			
	All soils	Sands	Silk	Clays
Imai and Yoshimura, 1970	$V_S = 76N^{0.33}$	–	–	–
Fujiwara, 1972	$V_S = 92.1N^{0.337}$	–	–	–
Ohsaki and Iwasaki, 1973	$V_S = 81.4N^{0.39}$	–	–	–
Imai et al., 1975	$V_S = 89.9N^{0.341}$	–	–	–
Imai, 1977	$V_S = 91N^{0.337}$	$V_S = 80.6N^{0.331}$	–	$V_S = 80.2N^{0.292}$
Ohta and Goto, 1978	$V_S = 85.34N^{0.348}$	–	–	–
Seed and Idriss, 1981	$V_S = 61.4N^{0.5}$	–	–	–
Imai and Tonouchi, 1982	$V_S = 96.9N^{0.314}$	–	–	–
Yokota et al., 1991	$V_S = 121N^{0.27}$	–	–	$V_S = 114N^{0.31}$
Kalteziotis et al., 1992	$V_S = 76.2N^{0.24}$	–	–	–
Pitilakis et al., 1992	–	$V_S = 162N^{0.17}$	–	$V_S = 165.7N^{0.19}$
Athanasopoulos, 1995	$V_S = 107.6N^{0.36}$	–	–	$V_S = 76.55N^{0.445}$
Raptakis et al., 1995		$V_S = 99.95N^{0.237}$	$V_S = 123.4N^{0.29}$	$V_S = 184.2N^{0.17}$
Lyisan, 1996	$V_S = 51.5N^{0.516}$	–	–	–
Pitilakis et al., 1999	–	$V_S = 145N^{0.178}$	–	$V_S = 132N^{0.271}$
Kiku et al., 2001	$V_S = 68.3N^{0.292}$	–	–	–
Jafari et al., 2002	$V_S = 22N^{0.85}$	$V_S = 19N^{0.85}$	–	$V_S = 27N^{0.73}$
Anbazhagan and Sitharam, 2006	$V_S = 50N^{0.41}$	–	–	–
Hasancebi and Ulusay, 2007	$V_S = 90N^{0.308}$	$V_S = 90.82N^{0.319}$	–	$V_S = 97.89N^{0.269}$
Hanumantharao and Ramana, 2008	$V_S = 82.6N^{0.43}$	$V_S = 79N^{0.434}$	$V_S = 86N^{0.42}$	–
Dikmen, 2009	$V_S = 58N^{0.39}$	$V_S = 73N^{0.33}$	$V_S = 60N^{0.36}$	$V_S = 44N^{0.48}$
Maheswari et al., 2010	$V_S = 95.64N^{0.3013}$	$V_S = 100.53N^{0.2651}$	–	$V_S = 89.31N^{0.3576}$
Mhaske and Choudhury, 2011	$V_S = 72N^{0.4}$	–	–	–
Thaker and Rao, 2011	$V_S = 59.72N^{0.42}$	$V_S = 51.21N^{0.45}$	–	$V_S = 62.41N^{0.42}$
Tsiambaos and Sabatakakis, 2011	$V_S = 136.6N^{0.275}$	$V_S = 92N^{0.341}$	$V_S = 99.45N^{0.364}$	$V_S = 140.1N^{0.290}$
Anbazhagan et al., 2013	$V_S = 68.96N^{0.51}$	$V_S = 60.17N^{0.56}$	–	$V_S = 106.63N^{0.39}$
Sun et al., 2013	$V_S = 65.64N^{0.407}$	–	–	–
Esfehanizadeh et al., 2014	$V_S = 107.2N^{0.34}$	–	–	–
Fabbrocino et al., 2015	$V_S = 90.35N^{0.317}$	–	$V_S = 149.3N^{0.192}$	$V_S = 110.5N^{0.252}$
Gautam, 2016	$V_S = 115.8N^{0.251}$	$V_S = 78.7N^{0.352}$	$V_S = 102.4N^{0.274}$	–
Kirar et al., 2016	$V_S = 95.5N^{0.345}$	$V_S = 100.3N^{0.338}$	–	$V_S = 94.4N^{0.379}$
Rahman et al., 2016	$V_S = 120.87N^{0.2501}$	–	–	–
Rahman et al., 2018	$V_S = 129.51N^{0.365}$	$V_S = 105.8N^{0.457}$	–	$V_S = 139.3N^{0.2835}$
This work, 2019	$V_S = 76.45N^{0.468}$	–	–	$V_S = 108.31N^{0.355}$

Since limited correlations between V_S and SPT-N for the soil sites in the HCMC areas and Viet Nam have been reported, the compatibility of the newly developed correlation with existing ones for other regions was assessed. Fig. 7a shows the V_S vs SPT-N plots for all soils obtained from this study and some previous reports in order to make an intuitive comparison among the results (Seed and Idriss, 1981; Lyisan, 1996; Hanumantharao and Ramana, 2008; Tsiambaos and Sabatakakis, 2011; Anbazhagan et al., 2013; Sun et al., 2013; Esfehanizadeh et al., 2014; Fabbrocino et al., 2015; Gautam, 2016). For all the data sets, the results of Tsiambaos et al. (SPT-N ≤ 20) and Anbazhagan et al. (SPT-N > 20) show the higher values, whereas those obtained by Sun et al. exhibit the lower ones (Anbazhagan et al., 2013; Tsiambaos and Sabatakakis, 2011; Sun et al., 2013). In the earlier work, Hanumantharao et al. reported the measurements of more than 80 boreholes (30 m of depth) in Delhi, India by using spectral analysis of surface waves (SASW) (Hanumantharao and Ramana, 2008). The V_S and SPT-N values were found in the range of 70–400 m/s and 3–50, respectively. Moreover, the values of a and b parameters determined from the equation (1) were 82.6 and 0.43, respectively. More recently, Anbazhagan et al. showed the measurements of more than 17 boreholes (30 m of depth) in Lucknow city, the central part of the Indo-Gangetic Basin of North India (Anbazhagan et al., 2013). The value of V_S, SPT-N, a, and b was found to be approximately 100–450 m/s, 3–50, 68.96, and 0.51, respectively by using the MASW method. Accordingly, our results are quite similar to those found by Hanumantharao et al. and Anbazhagan et al.; namely, the geological environments of these works exhibit the thick silty organic clay layer under the surface soil (Hanumantharao and Ramana, 2008; Anbazhagan et al., 2013). Fig. 7b shows the proposed empirical correlation for all clayey soils of this study and some previous works (Yokiota et al., 1991; Pitilakis et al., 1992; Athanasopoulos, 1995; Raptatis et al., 1995; Jafari et al., 2002; Maheswari et al., 2010; Tsiambaos and Sabatakakis, 2011; Kirar et al., 2016; Rahman et al., 2018). It can be noticed here that the correlation proposed in this study is comparable to those of some previous works in Fig. 7b and matches well with those reported by Tsiambaos and Sabatakakis, 2011; Kirar et al., 2016; and Rahman et al., 2018.

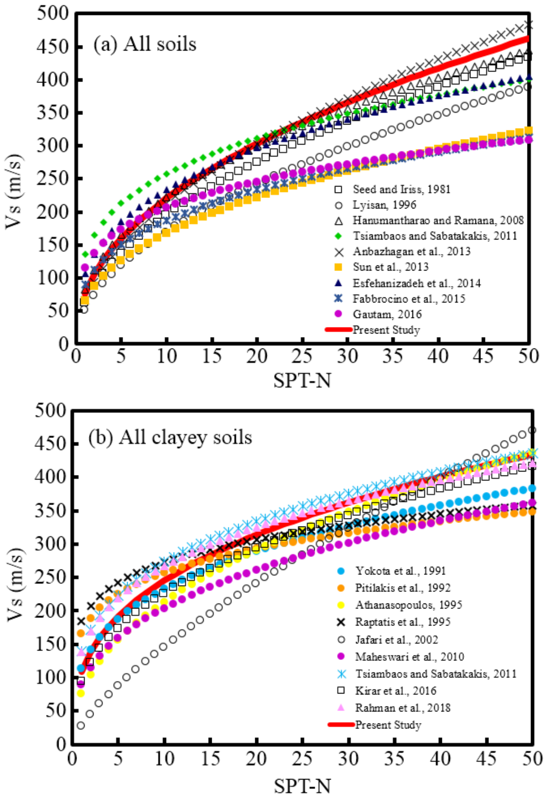

Fig. 7. The V_S vs SPT-N plots for this study and some previous reports for (a) all soils and (b) all clayey soils.

3.4 Comparison of shear wave velocity profiles and site classification

Fig. 8 represents the V_S profiles obtained by using the methods of MASW, downhole, and the empirical correlation of two sites of BH7 and PBH2 as a function of depth. The values of standard penetration test and the petrographic composition of boreholes are also showed in Fig. 8. It should be noted here that there are no reports to show such V_S profiles by using above different test methods, especially the MASW survey around HCMC areas and even in Viet Nam. For BH7 site (Fig. 8a), the shear wave velocities evaluated by using the downhole and MASW measurements are in the range of 69–398 and 68–400 m/s, respectively. Thus, the significant mismatch was observed at a depth of 4.6 m with the maximum difference and maximum relative difference of 22 m/s and 24%, respectively (Table 2). Moreover, the values of average relative difference, average difference, and standard deviation are 4%, 4.5%, and 5 m/s, respectively (Table 2). For PBH2 site (Fig. 8b), the shear wave velocities determined by the downhole and MASW measurements are in the range of 61–414 m/s and 61–415 m/s, respectively. Accordingly, the mismatch between two methods was observed at 12 m with the maximum difference of 8 m/s and at 3 m with maximum relative difference of 5.5%. Moreover, the values of average relative difference, average difference, and standard deviation are 3%, 3.3%, and 3 m/s, respectively (Table 2). For two borehole sites, the geological environments are classified into three layers. The first layer, corresponding to 0–1.5 m depth (a thickness of 1.5 m), having the V_S values of 75–93 m/s, is assigned to the filled soil. The second layer, corresponding to 1.5–12 m depth (a thickness of 10.5 m), having the V_S values of 61–200 m/s, is attributed to the soft organic silty clay. Finally, the third layer, corresponding to 12–30 m depth (a thickness of 18 m), showing the V_S values of 250–415 m/s, is ascribed to the firm clay soil.

The stiffness of soils obtained by the MASW method can be compared with that of N values from SPT. The values of SPT-N in the range of 0–2, 5–7, and 8–40, corresponding to the V_S values of 61–93 m/s, 157–200 m/s, and 250–415 m/s, are characterized by the soft filled soil near surface and soft silty clay layer, the silty clay, and the firm clay soil, respectively. It is observed that the behavior of V_S-depth profiles obtained by the MASW and downhole methods is similar with the average relative difference of 3–4%. The average relative difference of V_S by using the same methods reported previously is listed in Table 3. Based on these results, the obtained average relative difference of V_S in this study is quite small. Some reasons for this may relate to the number of boreholes used in the survey and their locations. In this study, the MASW measurements were conducted only at the two borehole sites (BH07 and PBH2), which are relatively close to each other. Moreover, the locations of the MASW surveys coincided with those of the borehole measurements. Therefore, it can be concluded that the obtained results in this study indicate the accuracy of the analysis methods and are sufficient for quantitative discussion.

In the next part, we represent the values of V_{S30} determined by using the methods of MASW, downhole, and empirical correlation between V_S and SPT-N. The values of V_{S30} obtained by using the MASW method for BH7 (150 m/s) and PBH2 (152 m/s) are very good agreement with those obtained by using the downhole measurements (151 and 150 m/s for BH7 and PBH2 sites, respectively). The V_{S30} values of 144 m/s for BH7 and 171 m/s for PBH2 determined by using the correlation between V_S and SPT-N are also in good agreement with those of the MASW and downhole measurements. Besides the V_{S30} values of BH7 and PBH2 sites as presented above, those of the other borehole sites were also estimated using the downhole method (137–161 m/s) and the empirical correlation (126–171 m/s). The relative differences of V_{S30} values estimated by all the methods are less than 14.8%. It can be noticed that the V_{S30} values calculated from above three methods are well classified as class E .

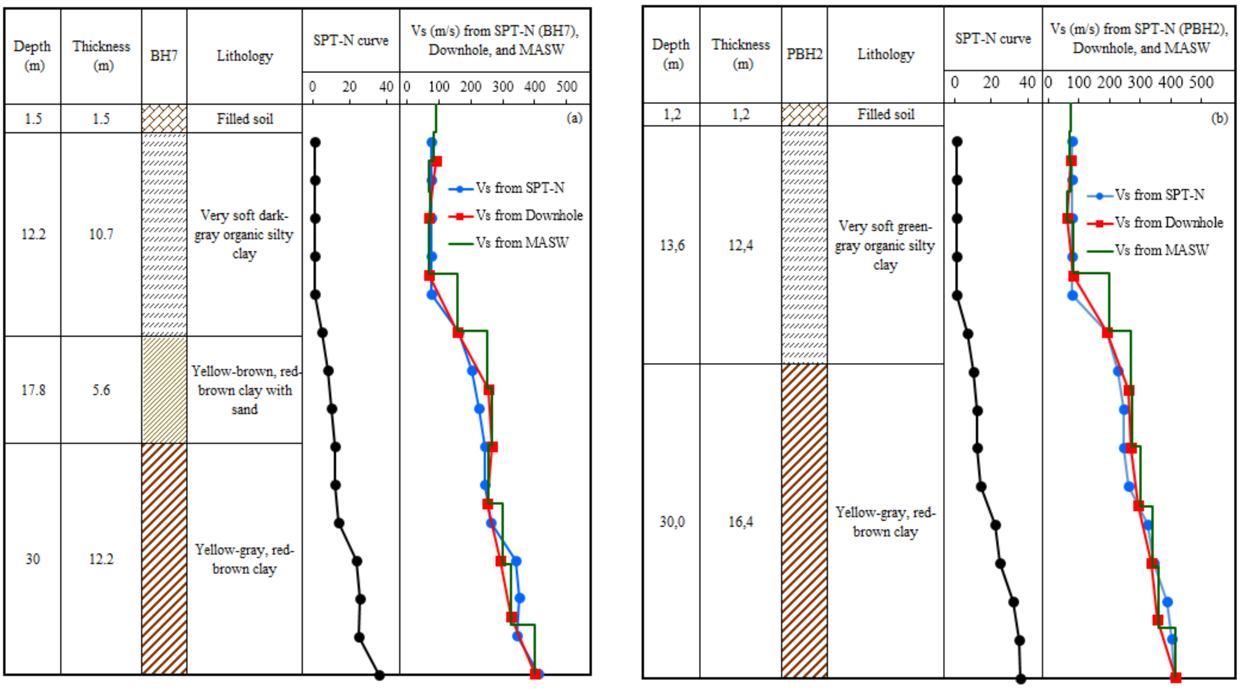

Fig. 8. Shear wave velocity profiles estimated by the methods of MASW, downhole seismic, and standard penetration test at the borehole sites of BH7 (a) and PBH2 (b).

Table 2. Comparison of V_S between the MASW and downhole measurements.

Borehole ID	Maximum difference (m/s)	Average difference (m/s)	Maximum relative difference (%)	Average relative difference (%)	Standard deviation (m/s)
BH07	22 at 4.6 m	4.5	24 at 4.6 m	4	5
PBH02	8 at 12 m	3.3	5.5 at 3 m	3	3

Table 3. The average relative difference of V_S between the MASW and borehole measurements of this study and some previous works.

Authors	Field investigations	Differences (%)
Xia et al., 2000	MASW/downhole	8–26%
Xia et al., 2002	MASW/downhole	~ 9–15%
Brown et al., 2002	SASW/borehole	~ 15%
Hunter et al., 2002	MASW/downhole	~ 9%
Stephenson et al., 2005	Remi, MASW/borehole	~ 15%
Thitimakorn, 2010	MASW/downhole	4–15%
Yilmaz et al., 2010	MASW/downhole	2–55%
Banab and Motazedian, 2010	MASW/borehole	4–20%
Fiore et al., 2015	MASW/downhole	26–47%
This work, 2019	MASW/downhole	3–4%

4. Conclusions

The stiffness of soil of the construction foundation at District 2 in Ho Chi Minh City was investigated by using the different test methods of MASW, downhole, and the empirical correlation. The geological environments within 30-m depth were divided into three layers. The first soft filled soil near surface has the V_S values of 75–93 m/s, corresponding to SPT-N values of less than 2. The second layer is soft organic silty clay having the V_S values of 61–200 m/s, corresponding to SPT-N values of 1–7. The third firm clay layer exhibits the V_S values of 250–415 m/s, corresponding to SPT-N values of 8–40. The average shear wave velocities obtained by the MASW, downhole, and empirical correlations methods are in the range of 150–152, 137–161, and 126–171, respectively. Consequently, the study area is well classified as class E according to the NEHRP. The results of the shear wave velocities and V_{S30} estimated by the MASW and downhole methods are similar with the average relative difference of 3–4%. The present study area possesses the thickness of the silty layer with larger than 10 m and the low V_S and V_{S30} values with less than 100 and 180 m/s, respectively, and thus representing an essential information to consider in the engineering constructions. The obtained results indicate that the MASW survey could be utilized to evaluate the stiffness of soil around HCMC areas. Moreover, the results have revealed more detailed geophysical features of soils in the study area, which can be utilized to develop a map of the stiffness of soil in HCMC. The next article in this series will consider the comparison of shear wave velocity profiles using the methods of MASW, downhole, and empirical correlations at Saigon High Tech Park of District 9 in HCMC.

Acknowledgements

This research is funded by Vietnam National University Ho Chi Minh City (VNU-HCM) under grant number C2019-18-03. We would like to thank Mr. Nguyen Van Luu and Mr. Vo Manh Khuong (South Vietnam Geological Mapping Division) for their supports the MASW and downhole experiments. The authors would like to thank Enago (www.enago.jp) for the English language review.

References

Abreu, A.E.S., Gandolfo, O.C.B. and Vilar, O.M., 2016. Characterizing a Brazilian sanitary landfill using geophysical seismic techniques. Waste Management, **53**: 116–127.

Anbazhagan, P. and Sitharam, T.G., 2006. Evaluation of dynamic properties and ground profiles using MASW: correlation between V_S and N_{60}. 13th Symposium on Earthquake Engineering, **13**: 8–18.

Anbazhagan, P., Parihar, A. and Rashmi, H.N., 2013. Seismic site classification and correlation between standard penetration test N value and shear wave velocity for Lucknow city in Indo-Gangetic Basin. Pure Applied Geophysics, **170**: 299-318.

Athanasopoulous, G.A., 1995. Empirical correlations Vs-N SPT for soils of Greece: A comparative study of reliability. Transactions on the Built Environment, **15**: 8–15.

Araffa, S.A.S., Atya, M.A., Mohamed, A.M.E., Gabala, M. and Zaher, M.A., 2014. Subsurface investigation on Quarter 27 of May 15th city, Cairo, Egypt using electrical resistivity tomography and shallow seismic refraction techniques. NRIAG journal of Astronomy and Geophysics, **3** (2): 170–183.

Banab, K.K. and Motazedian, D., 2010. On the efficiency of the multi-channel analysis of surface wave method for shallow and semideep loose soil layers. International Journal of Geophysics: 1–13.

Brown, L.T., Boore, D.M. and Stokoe, K.H., 2002. Comparison of shear-wave slowness profiles at 10 strong-motion sites from noninvasive SASW measurements and measurements made in boreholes. Bulletin of the Seismological Society of America, **92** (8): 3116–3133.

Dikmen, U., 2009. Statistical correlations of shear wave velocity and penetration resistance for soil. Journal of Geophysics and Engineering, **6**: 61–72.

Do, L.V. and Vo, K.M., 2017. Borehole seismic report of residential development project in Thu Thiem villas area, District 2, HCM City report. South Vietnam Geological Mapping Division.

Do, L.V., Thai, Q., Ha, H.T., Lai, T.V., Duong, C.C., Le, D.A., Dong, P.B., Pham, T.T. and Vu, T.A., 2018. Characteristic of structure and modern activity of Sai Gon river fault and implication for the ground subsidence and flooding in Ho Chi Minh City area. GEOSEA XV, **15**: 57–65.

Eker, A.M., Akgun, H. and Kockar, M.K., 2012. Local site characterization and seismic zonation study by utilizing active and passive surface wave methods: A case study for the northern side of Ankara, Turkey. Engineering Geology, **151**: 64–82.

Esfehanizadeh, M., Nabizadeh, F. and Yazarloo, R., 2014. Correlation between standard penetration (NSPT) and shear wave velocity (V_S) for young coastal sands of the Caspian Sea. Arabian Journal of Geoscience, **8**: 7333–7341.

Fabbrocino, S., Lanzano, G., Forte, G., Magistris, F.S. and Fabbrocino, G., 2015. SPT blow count vs. shear wave velocity relationship in the structurally complex formations of the Molise region (Italy). Engineering Geology, **187**: 84–97.

Fiore, V.D., Cavuoto, G., Tarallo, D., Punzo, M. and Evangelisa, L., 2015. Multichannel analysis of surface waves and down-hole tests in the archeological “Palatine Hill” area (Rome, Italy): Evaluation and influence of 2D effects on the shear wave velocity. Surveys in Geophysics, **37** (3): 625–642.

Fujiwara, T., 1972. Estimation of ground movements in actual destructive earthquakes. Proceedings of the Fourth European Symposium on Earthquake Engineering, London: 125–132.

Gautam, D., 2016. Empirical correlation between uncorrected standard penetration resistance (N) and shear wave velocity (V_S) for Kathmandu valley, Nepal, Geomatics. Natural Hazards and Risk Journal, **8**: 496–508.

Hanumantharao, C. and Ramana, G.V., 2008. Dynamic soil properties for microzonation of Delhi, India. Journal of Earth System Science, **117**: 719–730.

Hartantyo, E., Brotopuspito, K.K. and Waluyo, S., 2014. Comparison of 8 and 24 channels MASW data. Field performance: International Conference on Physics: 97–99.

Hasancebi, N. and Ulusay, R., 2007. Empirical correlations between shear wave velocity and penetration resistance for ground shaking assessments. Bulletin of Engineering Geology and the Environment, **66**: 203–213.

Haque, E.D.M., Kamal, M.A.S.M, Ullah, W.A.S.M. and Alam, B.Md., 2013. Comparison of shear wave velocity derived from PS logging and MASW – A case study of Mymensingh Pourashava, Bangladesh. Bangladesh Journal of Geology, **26**: 84–97.

Hunter, J.A., Benjumea, B., Harris, J.B., Miller, R.D., Pullan, S.E. and Good, R.L., 2002. Surface and downhole shear wave seismic methods for thick soil site investigations. Soil Dynamics and Earthquake Engineering, **22**: 931–941.

Imai, T. and Yoshimura, Y., 1970. Elastic wave velocity and soil properties in soft soil. Tsuchito-Kiso, **18**: 17–22.

Imai, T., Fumoto, H. and Yokota, K., 1975. The relation of mechanical properties of soil to P- and S-wave velocities in Japan. Proceedings of 4th Japan Earthquake Engineering Symposium: 89–96.

Imai, T., 1977. P and S wave velocities of the ground in Japan. Proceedings of IX International Conference on Soil Mechanics and Foundation Engineering, **2**: 127–132.

Imai, T. and Tonouchi, K., 1982, Correlation of N-value with S-wave velocity and shear modulus. Proceedings of the 2nd European Symposium of Penetration Testing, **2**: 57–72.

Jarari, M.K., Shafiee, A. and Razmkhah, A., 2002. Dynamic properties of fine grained soils in South of Tehran. Journal of Seismology and Earthquake Engineering, **4** (1): 25–35.

Kalteziotis, N., Sabatakakis, N. and Vassiliou, J., 1992. Evaluation of dynamic characteristics of Greek soil formations. Second Hellenic conference on Geotechnical Engineering: 92–100.

Kiku, H., et al., 2001. In-situ penetration tests and soil profiling in Adapazari. Proceedings of the ICSMGE/TC4 Satellite Conference on Lessons Learned From Recent Strong Earthquakes: 259–265.

Kirar, B., Maheshwari, B.K. and Muley, P., 2016. Correlation between shear wave velocity (V_S) and SPT resistance (N) for Roorkee region. International Journal of Geosynthetics and Ground Engineering, **1**: 1–11.

Lyisan, R., 1996. Correlations between shear wave velocity and in-situ penetration test results. Chamber of Civil Engineers of Turkey, **2**: 1187–1199.

Madun, A., Supa'at, M. E. A., Tajudin, S. A. S., Zainalabidin, M. H., Sani, S. and Yusof, M. F., 2016. Soil investigation using multichannel analysis of surface wave (MASW) and borehole. ARPN journal of engineering and applied sciences, **11**: 3759–3763.

Madun, A., Tajuddin, S.A.A., Abdullah, M.E., Abidin, M.H.Z., Sani, S., Siang, A.J.L.M. and Yusof, M.F., 2016. Conversion shear wave velocity to standard penetration resistance. Materials Science and Engineering, **136**: 1–7.

Mhaske, S.Y. and Choudhury, D., 2011. Geospatial contour mapping of shear wave velocity for Mumbai city. Natural Hazards, **59**: 317–327.

Maheswari, R.U., Boominathan, A. and Dodagoudar, G.R., 2010. Use of surface waves in statistical correlations of shear wave velocity and penetration resistance of Chennai soils. Geotechnical and Geological Engineering, **28**: 119–137.

Nguyen, T. N., 2004. Analyzing of geophysics data in Ho Chi Minh City: PhD thesis, University of Science, Viet Nam National University Ho Chi Minh City.

Nguyen, T. N., Vu, T. T. and Dinh, Q. T., 2014. Borehole seismic project at German house report. South Vietnam Geological Mapping Division.

Nguyen, T. N. and Vo, Q. T. H., 2015. Borehole seismic project at Saigon High Tech Park, District 9, Ho Chi Minh City report. South Vietnam Geological Mapping Division.

Nguyen, N. N. K., Nguyen, T. N. and Dinh, T. Q, 2015. Determining trans-horizontal velocity V_S and elastic parameters of rock and soil by multichannel surface wave method. Journal of Geology, General Department of Geology and Minerals of Vietnam, **352–353**: 229–237.

Nguyen, H. K. and Phienwej, N., 2016. Practice and experience in deep excavations in soft soil of Ho Chi Minh City, Vietnam. Journal of Civil Engineering, **20** (6): 2221–2234.

Nguyen, B. T., Samsura, D. A. A., Kraben, E. and Le, D. A., 2016. Saigon-Ho Chi Minh City. Cities, **50**: 16–27.

Nguyen, T. N., Dinh, Q. T. and Vo, K. M., 2016. Borehole seismic project at Long Phu thermal power plant, Thanh Duc hamlet, Long Duc commune, Long Phu district, Soc Trang province report. South Vietnam Geological Mapping Division.

Ohsaki, Y. and Iwasaki, R., 1973. On dynamic shear moduli and Poisson's ratio of soil deposits. Soil Found, **13**: 61–73.

Ohta, Y. and Goto, N., 1978. Empirical shear wave velocity equations in terms of characteristic soil indexes. Earthquake engineering and structural dynamics, **6**: 167–187.

Pamuk, E., Ozdag, O. C., Ozyalin, S. and Akgun, M., 2017. Soil characterization of Tinaztepe region (Izmir/Turkey) using surface wave methods and Nakamura (HVSR) technique. Earthquake Engineering and Engineering Vibration, **16** (2): 447–458.

Park, C. B., Miller, R. D. and Xia, J., 1999. Multichannel analysis of surface waves. Geophysics, **64**: 800–808.

Park, C.B. and Ryden, N., 2007. Historical overview of the surface wave method. Symposium on the Application of Geophysics to Engineering and Environmental Problems: 897–909.

Pitilakis, K.D., Anastassiadis, A. and Raptakis, D., 1992. Field and laboratory determination of dynamic properties of natural soil deposits. The 10th Earthquake Engineering conference proceedings: 1275–1280.

Pitilakis, K., Raptakis, D., Lontzetidis, K., Tika-Vassilikou, Th. And Jongmans, D., 1999. Geotechnical and geophysical description of Euro-seistest, using field, laboratory tests and moderate strong motion recordings. Journal of Earthquake Engineering, **3** (3): 381–409.

Raef, A., Gad, S. and Tucker-Kulesza, S., 2015. Multichannel analysis of surface-waves and integration of downhole acoustic televiewer imaging, ultrasonic V_S and V_P, and vertical seismic profiling in an NEHRP-standard classification, South of Concordia, Kansas, USA. Journal of Applied Geophysics, **121**: 149–161.

Rahman, Md.Z., Siddiqua, S. and Kamal, A.S.M.M., 2016. Shear wave velocity estimation of the near-surface materials of Chittagong city, Bangladesh for seismic site characterization. Journal of Applied Geophysics, **134**: 210–225.

Rahman, Md.Z., Hossain, Md.S., Kamal, A.S.M.M., Siddiqua, S., Mustahid, F. and Farazi, A.H., 2017. Seismic site characterization for Moulvibazar town, Bangladesh. Bulletin of Engineering Geology and the Environment, **7** (77): 1451–1471.

Rahman, Md.Z., Kamal, A.S.M.M. and Siddiqua, S., 2018. Near-surface shear wave velocity estimation and V_S^{30} mapping for Dhaka City, Bangladesh. Natural Hazards, **92** (3): 1687–1715.

Raptakis, D.G., Anastasiadis, A.J., Pititakis, K.D. and Lontzetidis, K.S., 1995. Shear wave velocities and damping of Greek natural soils. The 10th European Conference on Earthquake Engineering proceedings, **1**: 477–482.

Rehman, F., El-Hady, S., Atef, A.H. and Harbi, H.M., 2016. Multichannel analysis of surface waves (MASW) for s eismic site characterization using 2D genetic algorithm at Bahrah area, Wadi Fatima, Saudi Arabia. Arabian Journal of Geosciences, **9**: 519–532.

Seed, H.B. and Idriss, I.M., 1981. Evaluation of liquefaction potential sand deposits based on observation of performance in previous earthquakes. ASCE National Convention (MO): 481–544.

Stephenson, W. J., Louie, J. N., Pullammanappallil, R. A., Williams, J.K. and Odum, J. K., 2005. Blind shear-wave velocity comparison of ReMi and MASW results with boreholes to 200 m in Santa Clara valley: Implications for Earthquake Ground-Motion Assessment. Bulletin of the Seismological Society of America, **95** (6): 2506–2516.

Sun, C. G., Cho, C. S., Son, M. and Shin, J. S., 2013. Correlations between shear wave velocity and in-situ penetration test results for Korean soil deposits. Pure and Applied Geophysics, **170**: 271–281.

Thaker, T.P. and Rao, K.S., 2011. Development of statistical correlations between shear wave velocity and penetration resistance using MASW technique. Pan-Am CGS Geotechnical Conference.

Thitimakorn, T., 2010. Comparison of shear-wave velocity profiles of Bangkok subsoils from multi-channel analysis of surface wave and downhole seismic methods. Journal of Applied Sciences Research, **6**: 1953–1959.

Trupti, S., Srinivas, K.N.S.S.S., Kishore, P.P. and Seshunarayana, T., 2012. Site characterization studies along coastal Andhra Pradesh-India using multichannel analysis of surface waves. Journal of Applied Geophysics, **79**: 82–89.

Tsiambaos, G. and Sabatakakis, N., 2011. Empirical estimation of shear wave velocity from in situ tests on soil formations in Greece. Bulletin of Engineering Geology and the Environment, **7**: 291–297.

Vu, C. D. and Do, L. V., 2018. Primarily analyzing of DEM model to recognize active traces of river Sai Gon fault during late Pleistocen-Holocen Period in Ho Chi Minh City area. Journal of Science and Technology Development, **11**: 13–21.

Xia, J., Miller, R. D., Park, C. B., Hunter, J. A. and Harris, J. B., 2000. Comparing shear-wave velocity profiles from MASW with borehole measurements in unconsolidated sediments, Fraser river delta, B.C., Canada. Journal of Environmental & Engineering Geophysics, **5** (3): 1–13.

Xia, J., Miller, R. D., Park, C. B., Hunter, J. A., Harris, J. B. and Ivanov, J., 2002. Comparing shear-wave velocity profiles inverted from multichannel surface wave with borehole measurements. Soil Dynamics and Earthquake Engineering, **22**: 181–190.

Yilmaz, O., Eser, M., Sandikkaya, A., Akkar, S., Bakir, S. and Yilmaz, T., 2008. Comparison of shear wave velocity depth profiles from downhole and surface seismic experiments. Proceedings of the 14th WCEE, Beijing, China.

Yokota, K., Imai, T. and Konno, M., 1991. Dynamic deformation characteristics of soils determined by laboratory tests. OYO Tec., **3**: 13–37.

Symbols and abbreviations

a, b	Coefficients of empirical function
d_i	Thickness of the ith layer
NEHRP	National earthquake hazards reduction program guidelines
MASW	Multichannel analysis of surface wave
R	Correlation coefficient
SPT-N	Standard penetration test blow counts
V_S	Shear wave velocity
V_{S30}	Average shear wave velocity
V_{si}	Shear wave velocity of the i^{th} layer
X_i	Source offsets